HIGH-CYCLE FATIGUE EFFECTS OF AN ELECTRON-BEAM COSMETIC PASS OR A GAS-TUNGSTEN-ARC WELD OVERLAY ON MICROFISSURED ALLOY 718

Stephen W. Holcomb and Donald F. Atkins

Rockwell International/Rocketdyne Division
Canoga Park, California 91303

Abstract

A high-cycle fatigue program was performed and consisted of testing the following conditions: (1) nonmicrofissured, (2) microfissured, (3) microfissured with subsequent electron beam cosmetic pass, and (4) microfissured with subsequent gas-tungsten-arc weld overlay. The nonmicrofissured condition resulted in an endurance strength of 120 ksi at 10^7 cycles. Scanning electron microscope examination of the fractured surfaces revealed initiation sites at carbides. This provided a baseline for comparing subsequent testing. Specimens containing microfissures showed an endurance limit of 60 ksi at 10^7 cycles. Scanning electron microscope examination of the fractured surfaces confirmed that initiation was at the site of a microfissure. Both the electron beam cosmetic pass and the gas-tungsten-arc weld overlay over existing microfissures improved fatigue strength. However, the electron beam cosmetic pass resulted in a substantial increase, while the gas-tungsten-arc weld overlay specimens resulted in only a modest increase. Endurance strengths at 10^7 cycles were 97 ksi and 74 ksi, respectively. Scanning electron microscope examination of these specimens showed much smaller microfissures when compared to the microfissure specimens.

Superalloy 718—Metallurgy and Applications
Edited by E.A. Loria
The Minerals, Metals & Materials Society, 1989

Introduction

Alloy 718, a nickel-based superalloy, is used extensively on the Space Shuttle Main Engine (SSME). It accounts for about 50% of the total engine weight. In many applications, components of Alloy 718 are electron beam welded. By design, Alloy 718 is one of the most weldable precipitation-hardened superalloys. The addition of niobium (~5%) delays the gamma prime formation, thereby reducing post-weld strain age cracking. However, the niobium addition is believed to be associated with grain boundary liquation in the heat-affected zone (HAZ). This localized melting can, under certain circumstances, lead to grain boundary separation during cooling of the weldment. These grain boundary separations are called "microfissures." To further complicate the problem, microfissures are not detectable using current nondestructive testing (NDT) techniques.

Although microfissuring in Alloy 718 welds has been investigated for over 25 yr, a complete understanding of the mechanism has yet to be determined. Microfissuring in Alloy 718 has been observed in electron beam (EB) welded components of the SSME; therefore, it is important that the microfissuring effect on mechanical properties be known.

Test Procedure

Material

Plate stock for the high-cycle fatigue (HCF) test program was obtained in two different thicknesses (1/4 and 3/8 in.). Heat chemistry and properties, as reported by vendor certifications, are shown in Table I. The 1/4-in. plate stock was received in the 1750°F solution heat-treated condition and had a fine grain size (ASTM 8). The 1/4-in. plate stock was used to weld specimens for the zero microfissure condition. It was found that a small grain size, combined with a 1750°F solution heat treatment prior to welding, can significantly reduce microfissuring. The 3/8-in. plate stock was received in the 1900°F solution heat-treated condition and had a grain size of ASTM 5. The 3/8-in. plate stock was used for the following tests: fissured, fissured with a subsequent EB cosmetic pass, and fissured with a subsequent gas-tungsten-arc weld (GTAW) overlay.

Welding

It was necessary to develop EB weld parameters suitable for producing HAZ microfissures in wrought Alloy 718. This was accomplished by using either a double-pass or triple-pass bead on plate EB weldment. Test panels 1/4 by 6 by 18 in. and 3/8 by 6 by 18 in. were EB welded in the as-received condition to produce a no microfissure and microfissure condition, respectively. Weld parameters for each test condition are shown in Table II.

A 30-kW, 500-mA/60-kV capacity Sciaky EB welder was used to apply the bead on plate EB welds along the 18-in. length of the panel.

Table I. Test Material - Vendor Certifications

Plate Stock Thickness (in.)	Heat No.	Composition (wt.%)												
		C	Mn	Fe	Ni	Cr	Al	Ti	Co	Mo	Cb+Ta	S	Si	Cu
0.250	Cabot 2180-3-9985	0.06	0.16	Bal	52.95	18.16	0.54	0.83	0.15	3.03	5.07	<0.002	0.15	0.03
0.375	Huntington HT26K5EK	0.04	0.15	17.39	53.93	18.24	0.52	0.98	0.24	2.93	5.03	0.001	0.25	0.29

		Mechanical Properties - Room Temperature[a]			
		F_{tu} (ksi)	F_{ty} (0.2%)(ksi)	Elongation (%)	Grain Size (ASTM No.)
0.250	Cabot 2180-3-9985	195	162	22	5[b]
0.375	Huntington HT26K5EK	196	162	24	5

[a]Material heat treated per RBO-170-154 (1900°F, 20 min, air cool; 1400°F, 10 h; furnace cool to 1200°F, air cool)
[b]ASTM-8 as-delivered

Table II. Weld Parameters[a]

Specimen Identification	Specimen Gage Thickness (in.)	Welded Panel				
		Thick-ness (in.)	Speed (ipm)	kV	mA	No. of Passes
No microfissures						
8-XX	0.125	0.250	25	45	70	1
Microfissures						
11-XX 32-XX	0.250	0.375	30	50	130	2
13-XX 31-XX	0.250	0.375	30	50	130	3
EB cosmetic pass						
31B-XX 32B-XX	0.200	0.375	10.0	45	40	1
GTAW overlay				Pulsed	Pulsed	
31A-XX 32A-XX	0.200	0.375	3.0	8.6/8.2 V	100×10^3/ 60×10^3	1

[a]Reference 7.

Specimens to be HCF tested with a subsequent EB cosmetic pass or a GTAW overlay were further processed as follows.

1. EB weld beads from four test panels, two double pass and two triple pass, were flushed to the surface.

2. Using a 1-in.-wide mill cutter, metal was removed to a depth of 0.050 in. along the full 18-in. length of the weld. The cutter was positioned so that the weld was in the center of the 1-in.-wide milled-out section (Figure 1).

3. Dye-penetrant examination was performed in the 1-in.-wide milled section to verify the presence of exposed microfissures.

4. An EB cosmetic pass was performed over the existing weld of one double-pass and one triple-pass panel.

5. A GTAW overlay also was performed over one double-pass and one triple-pass panel.

6. Parameters for both the EB cosmetic pass and GTAW overlay are shown in Table II.

Specimen Fabrication

Specimen blanks, 1.5 in. wide by 6.0 in. long, were sectioned from the weld panels. The welds spanned the 1.5-in. dimension at the center of the 6.0-in. length so that, on finished specimens, the welds were situated at the center of the gage section. Weld beads were first ground flush with the parent metal surface for each condition tested. Specimens in the non-microfissured and microfissured conditions were then ground down 0.050 in. to expose microfissures in the nail-head region of the weld. The back surfaces were then ground to obtain final specimen thicknesses (see Table II). The final machined specimens can be seen in Figure 1.

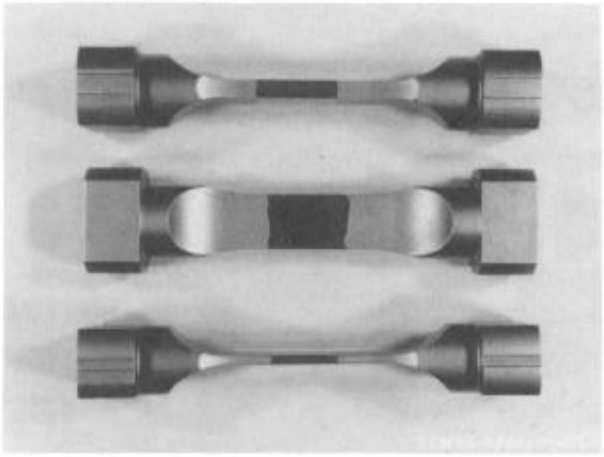

Figure 1 - 1/4 in. and 1/8 in.
final machined specimens

Post-Fabrication Heat Treatment

The post-fabrication heat treat cycle consisted of a 1900°F solution anneal for 25 min followed by an aging at 1400°F for 10 h and 1200°F for a total aging time of 20 h.

Metallography

A metallographic examination was performed to see the microstructural effects of the EB cosmetic pass and the GTAW overlay. A metallographic examination also was performed on the no microfissure and microfissure panels to verify the no microfissure and microfissure conditions. Figures 2 through 5 show typical transverse sections of welds for each condition tested. The photographs reveal the material in the post-weld solution annealed and aged condition.

Testing

Fatigue tests were conducted using closed-loop servohydraulic test frames. Special specimen grips were used that applied circumferential pressure to the grip area. These grips reduced the loading stress on the specimen ends and eliminated failures in the grip region of the specimens. Periodic alignment checks were made during test setups.

All of the HCF tests were performed at room temperature, in an air environment, under tension-tension axial loading. The ratio of minimum/maximum stress was 0.6 (R = 0.6) at cyclic frequencies of 15 Hz. Applied loads were set within $\pm$12 lb of the intended value, and stress levels were selected to provide fatigue failures over the 10^5 to 10^7 cycle range.

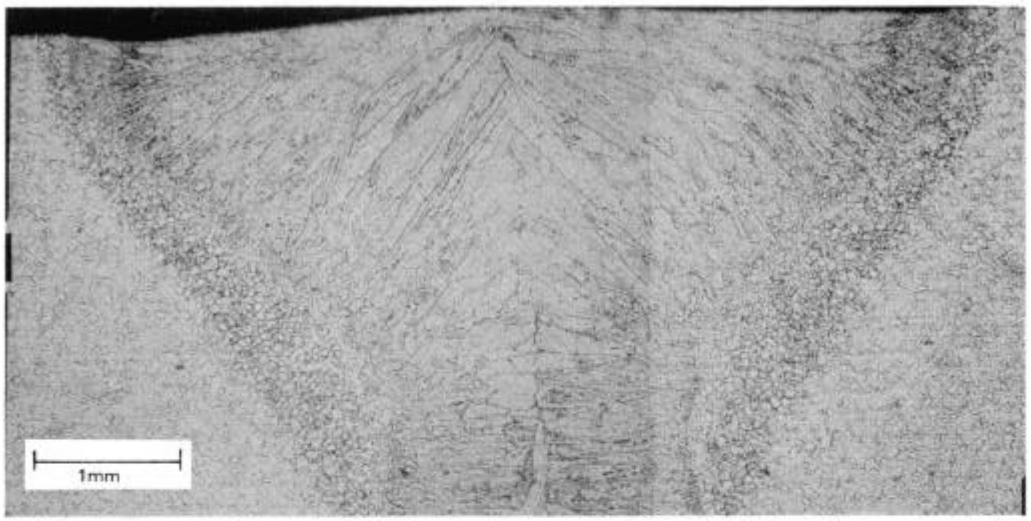

Figure 2 - Transverse cross section of
no-microfissure condition

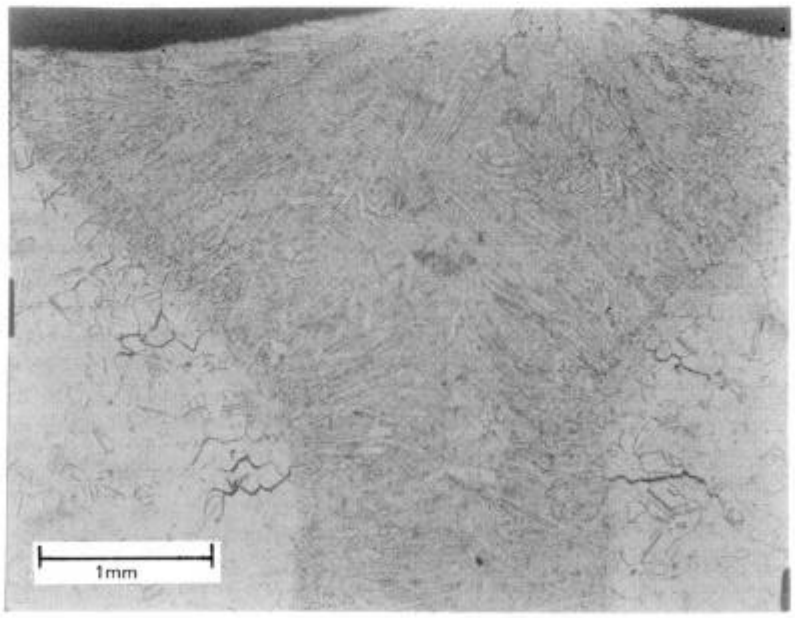

Figure 3 - Transverse cross section
of microfissure condition

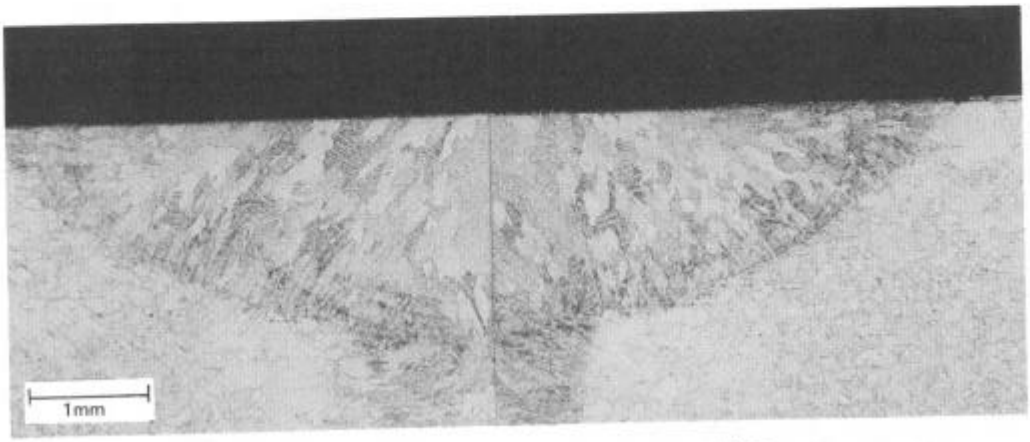

Figure 4 - Transverse cross section
of EB cosmetic pass condition

Figure 5 - Transverse cross section of
GTAW overlay condition

Results

High-cycle fatigue test data for nonmicrofissured, microfissured, EB cosmetic pass, and GTAW overlay conditions are shown in Table III.

Table III. High-Cycle Fatigue EB-Welded Inconel 718

Condition	Specimen Identification	Maximum Stress (ksi)	Cycles, Nf (X 1000)
No microfissures	8-10	150	430.3
	8-05	150	340.9
	8-02	142	995.1
	8-03	142	520.8
	8-04	132	1,728.7
	8-07	130	662.8
	8-09	125	4,004.1
	8-01	121.8	2,160.9
Microfissures	25-12	110	170.7
	25-16	90	371.0
	25-18	90	555.0
	25-20	90	377.0
	25-4	85	700.0
	25-2	80	760.0
	25-15	75	1,230.0
	25-14	70	1,010.0
	25-6	70	1,291.0
	25-17	65	10,200.0*
	25-3	65	6,030.0
	25-13	60	10,030.0*
EB cosmetic pass	31B-3	140	276.7
	32B-5	130	1,665.9
	31B-4	120	721.3
	32B-7	110	6,678.5
	31B-2	110	1,047.2
	31B-1	100	1,895.9
	32B-8	100	2,296.7
	32B-6	95	10,246.4*
GTAW overlay	31A-5	110	321.6
	32A-4	110	302.3
	31A-6	100	351.2
	31A-9	100	307.8
	32A-1	90	1,355.1
	31A-7	90	677.2
	31A-8	88	2,392.2
	32A-3	85	10,035.7*
	32A-2	80	10,005.6*

*Specimen removed from test frame before failure occurred.

Nonmicrofissured Specimens

The HCF tests were performed on EB-welded Alloy 718 with no microfissures. These tests provided a baseline for comparing microfissured welds. The S/N curve, Figure 6, shows an endurance strength of 120 ksi at 10^7 cycles. Scanning electron microscope examination was used to examine the fractured surfaces. The examination revealed that failure initiated in the HAZ of the weld and that there were no microfissures on the fractured surface. Figure 7 shows a typical nonmicrofissured fracture surface with initiation starting at a carbide.

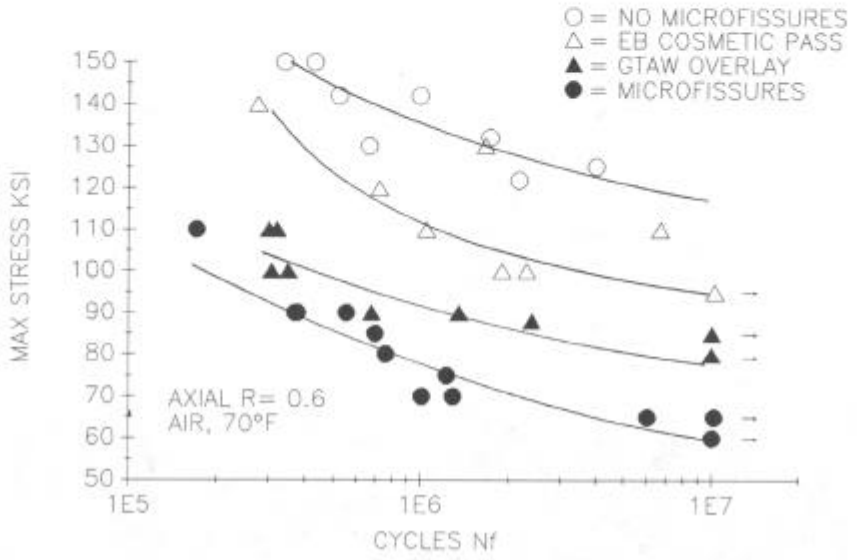

Figure 6 - High-cycle fatigue based on least-squares fit (axial, R = 0.60, air, 70°F)

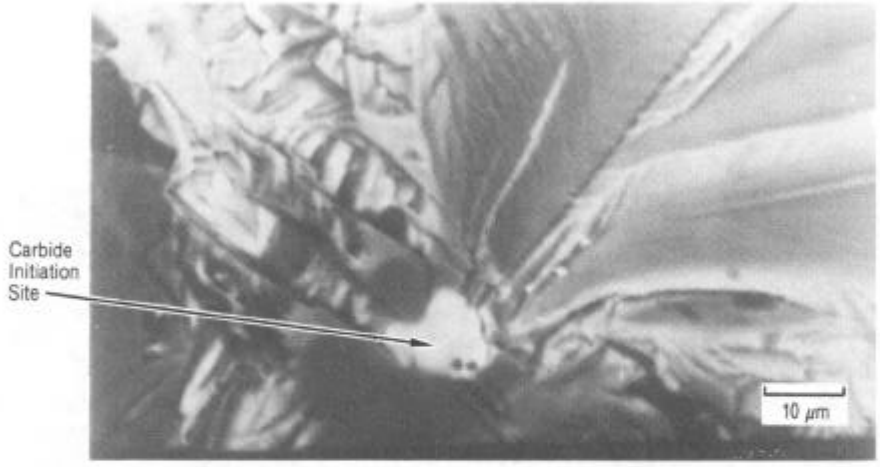

Figure 7 - Scanning electron microscope fractography of no-microfissure condition. Arrow points to carbide initiation site.

Microfissured Specimens

Data obtained from the microfissured HCF tests show an endurance strength of 60 ksi at 10^7 cycles. This suggests that weld-related microfissures, when exposed to the surface, reduce the fatigue strength of EB-welded Alloy 718 by 50%, as compared with nonmicrofissured Alloy 718. The S/N curve for these data is shown in Figure 6. The SEM examination revealed that initiation started at a microfissure for each specimen tested. Energy dispersive X-ray analysis (EDAX) of the microfissure surface showed them to be high in niobium and nickel. This observation supports the theory that grain boundary melting in the HAZ during EB welding is the result of a nickel-niobium eutectic formation.

Occasionally, secondary cracking that extended into the specimen was visible around the microfissure initiation sites. The secondary cracks ran intergranularly and had the characteristic nodular appearance of a microfissure. An EDAX of the surface confirmed that the secondary cracks were identical in chemical composition to the microfissure initiation sites. Propagation of these secondary cracks was not observed. This is believed to be caused by the orientation of the secondary cracks that were parallel to the load. Figure 8 shows a typical microfissure initiation site. The microfissure, outlined in black, has a surface exposed length of 0.015 in. However, the exposed length does not always reflect the magnitude and/or orientation of the microfissure internally.

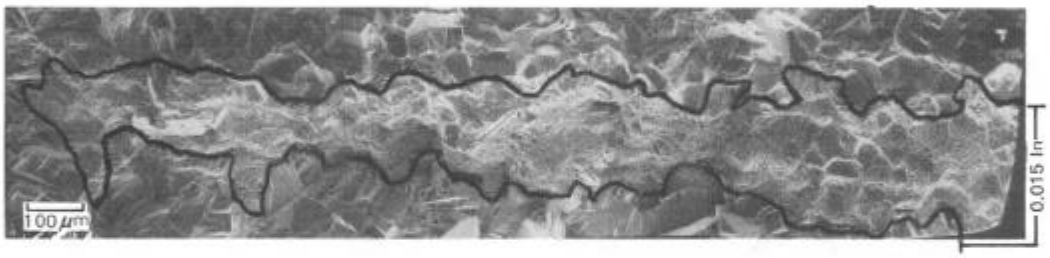

Figure 8 - Scanning electron microscope fractography of microfissure condition. Arrow points to exposed microfissure initiation site.

Microfissures with a Subsequent EB Cosmetic Pass

High-cycle fatigue test data obtained from microfissured specimens with a subsequent EB cosmetic pass showed an endurance strength (σ max) of 97 ksi at 10^7 cycles. The S/N curve for these data is shown in Figure 6. This is approximately a 60% increase in fatigue strength when compared to specimens without the EB cosmetic pass (i.e., microfissure specimens). However, the increase in fatigue strength resulting from the EB cosmetic pass did not reach that of the no-microfissure specimens.

SEM examination of the fractured fatigue specimens revealed that initiation was at the sites of microfissures. Initiation was generally internal, and the size of the microfissure was much smaller than those seen in the microfissure specimens. Figure 9 shows a typical initiation site of a microfissure specimen that received an EB cosmetic pass.

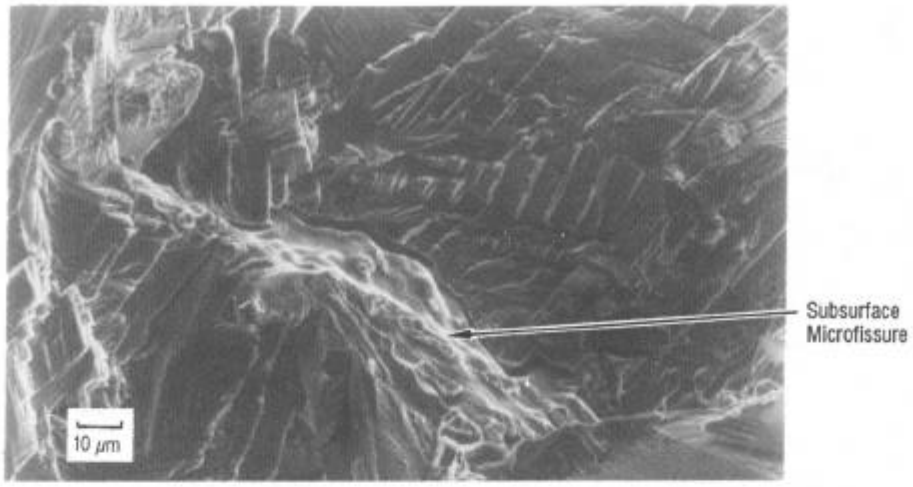

Figure 9 - Scanning electron microscope fractography of EB cosmetic pass condition. Arrow points to subsurface microfissure initiation site.

Microfissures with a Subsequent GTAW Overlay

High-cycle fatigue test data obtained from microfissured specimens that received a subsequent GTAW overlay showed an endurance strength of 74 ksi at 10^7 cycles. The S/N curve for these test data is shown in Figure 6. As shown, this curve is somewhat lower than the S/N curve for microfissures with a subsequent EB cosmetic pass. However, when the curve is compared to the microfissure specimens, an increase in fatigue strength at 10^7 cycles is evident.

A SEM examination of the fractured fatigue specimens revealed that initiation was at the site of microfissures. These initiation sites, like the EB cosmetic pass specimens, were generally internal. The size of the initiation sites fell somewhere between the microfissure specimens and the EB cosmetic pass specimens. An edge microfissure initiation site found on a GTAW overlay specimen is shown in Figure 10.

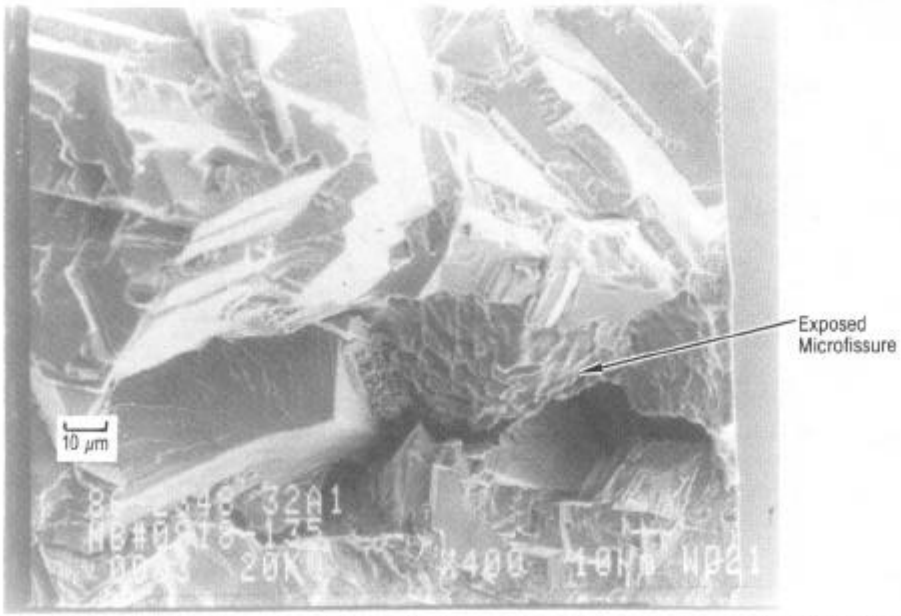

Figure 10 - Scanning electron microscope fractography of GTAW overlay condition. Arrow points to edge initiated microfissure.

Conclusions

Following are the conclusions drawn from the testing:

a) A reduction in fatigue strength of 50% at 10^7 cycles was observed for EB-welded Alloy 718 with surface-exposed microfissures, as compared to EB-welded Inconel 718 with no microfissures. This change suggests that microfissures act as HCF crack initiation sites and measurably reduce fatigue strength.

b) The microfissures were generally located in the transition region between the nail head and the stem of an electron-beam weld.

c) When an EB cosmetic pass was applied over surface-exposed microfissures, an increase of 60% in fatigue strength was observed.

d) When a GTAW overlay was applied over surface exposed microfissures, an increase of 20% in fatigue strength was observed.

e) The difference in fatigue strength between the EB cosmetic pass specimens and the GTAW overlay specimens is believed to be caused by the depth of penetration between the two processes. This is significant because if the depth of penetration is not sufficiently deep to remelt the microfissures that reside in the transition region, between the nail head and the stem, an increase in fatigue strength will not be realized.

f) If microfissuring occurs in the stem of the weld, an EB cosmetic pass or GTAW overlay would not be expected to improve fatigue strength.

References

1. R. G. Thompson, A Generalized Theory of HAZ Microfissuring Susceptibility in Nb-Bearing Alloys, University of Alabama at Birmingham.

2. R. G. Thompson and S. Genculu, "Microstructural Evolution in the HAZ of Inconel 718 and Correlation with the Hot Ductility Test Welding," Research Supplement, December 1983, 3375-3453.

3. W. Yeniscavich, "The Effects of Fissures on the Fatigue Strength of Ni-Cr-Fe Alloys," AWS: Welding, Research Supplement, March 1966, 111-S to 123-S.

4. T. T. Morrison, "Investigation of Weld Heat-Affected Zone Microfissuring in Alloy 718," MPTR-7-176A-8, Rocketdyne Division, Rockwell International, Canoga Park, CA.

5. D. H. Lassilla, "High-Cycle Fatigue Testing of Inconel 718 EB Weldments with Microfissures," Rocketdyne, MPR-81-0401, SSME 81.0996, April 10, 1981.

6. D. F. Atkins, "Interim Report, the Effect of Weld-Related Microfissures on the High-Cycle Fatigue Life of EB-Welded Inconel 718, RSS-8746, Rocketdyne, NASA Special Task Assignment No. 162.

7. G. Snyder, "Welding Development of Inconel 718, Preselected Microfissure Lengths," Kingsbury Task K3B/1.

5687a/sjv